JOURNAL OF MATERIALS SCIENCE **38** (2003) 261 – 267

Non-equilibrium grain boundary co-segregation of Boron and Magnesium in Ni_3Al

DONGLIANG LIN
School of Materials Science and Engineering, Shanghai Jiao Tong University, Shanghai 200030, People's Republic of China
E-mail: dqli@maill.sjtu.edu.cn

JING HU
School of Materials Science and Engineering, Shanghai Jiao Tong University, Shanghai 200030, People's Republic of China; Department of Mechanical and Engineering, Jiangsu Institute of Petrochemical Technology, Changzhou 213016, People's Republic of China

YUN ZHANG
School of Materials Science and Engineering, Shanghai Jiao Tong University, Shanghai 200030, People's Republic of China

The non-equilibrium grain boundary co-segregation of boron and magnesium in Ni_3Al–B–Mg alloys was determined by Auger electron spectroscopy (AES) in conjunction with ion sputtering in a cooling rate range of 0.05–269 K/s from temperatures of 1023, 1223 and 1373 K. The analytical expressions of diffusion rate equations describing non-equilibrium segregation process based on the concept that mobile solute-vacancy complexes migrating to grain boundaries is responsible for non-equilibrium grain boundary segregation of solute atoms in an alloy was used to simulate well the experimental results. The diffusion coefficients for boron atoms, boron-vacancy complexes, magnesium atoms and magnesium-vacancy complexes were determined, and the binding energy of boron-vacancy and magnesium-vacancy complexes was estimated.

1. Introduction

The ductilization effect for intermetallic compound Ni_3Al by small amount of boron addition is directly related to grain boundary segregation of boron [1]. Previous Work [2–4] has shown that grain boundary segregation of boron in Ni_3Al is an equilibrium process. Recently, in our laboratory, a non-equilibrium grain boundary segregation of boron in Ni_3Al–B alloys was determined by Auger electron spectroscopy (AES) [5]. Further work [6] showed that a small amount of magnesium can increase the ductility of boron-doped Ni_3Al alloys both at room and high temperature, which was suggested to be related to the enhancement of grain boundary segregation of boron by magnesium addition. In this paper, the non-equilibrium grain boundary co-segregation of boron and magnesium was determined by AES in conjunction with ion sputtering in Ni_3Al–B–Mg alloys. The analytical expression [7, 8] of diffusion rate equations describing non-equilibrium segregation process based on the concept that mobile solute-vacancy complexes diffusing to grain boundaries (vacancy sinks) is responsible for the non-equilibrium grain boundary segregation of solute atoms in alloys was used to simulate the experimental results.

2. Experimental

Two alloys of Ni_3Al-0.0944at%B-0.0210at%Mg and Ni_3Al-0.09994at%B-0.0840at%Mg were used in this work. The alloys were prepared by induction melting and directionally solidifying under a vacuum of 4×10^{-3} Pa. The resulting alloy plates were homogenized at 1373 K in air for 48 hrs followed by furnace cooling. The specimens of notched round bar for AES measurements were cut from the directionally solidified (DS) alloy plates and the long dimension of specimen is perpendicular to the growth direction of DS alloys. The AES specimens were annealed in a quartz tube under vacuum of 10^{-3} Pa for 48 hrs at 1023, 1223 and 1373 K respectively and cooled to room temperature under three cooling rates of 269, 4.5 and 0.05 K/s from each annealing temperature.

Grain boundary segregation profiles of boron and magnesium were determined by a PH600-type AES instrument in conjunction with ion sputtering where the boron concentration was measured by Auger-peak-height ratio (PHR), and the related test conditions were listed: 3 kV electron accelerated voltage, 2–2.06 $\times$ 10^{-7} A electron current, 6.1×10^{-8} Pa vacuum, 30° electron incident angle, 4 kV ion accelerated voltage

and 218–220 μA/cm^2 ion current density. Under those conditions an argon ion sputtering rate of 0.219 nm/s was determined. On the intergranularly fractured surface for each specimen, 5 to 6 points in different grain boundaries were analyzed and the resulting data given were the average values. A quantitative AES with matrix effect correction based on the relative sensitivity factor [9–11], which is a new quantitative Auger analysis without standard materials, was used in this study [12]. The boron and magnesium profiles can be obtained directly from the measured PHR values of the differential AES.

3. Theoretical expressions

Based on the concept [13–16] that mobile solute-vacancy complexes migrating to grain boundaries (vacancy sink) is responsible for the non-equilibrium grain boundary segregation of solute atoms in alloys and the driving force for the annihilation of vacancies at grain boundaries during cooling from initial temperatures, an analytical expression was put forward [7, 8]. The solution for the three coupled diffusion equations of free vacancies, free solutes and solute-vacancy complexes satisfying boundary conditions, and initial and initial boundary conditions were derived as [7, 8]

$$C_{\mathrm{V}}^{\mathrm{f}} = A''(T_{\mathrm{i}}) + [A''(T) - A''(T_{\mathrm{i}})]\mathrm{erf}\frac{x}{2\sqrt{D_{\mathrm{V}}^{\mathrm{f}}t}} \tag{1}$$

$$\begin{aligned} C_{\mathrm{S}}^{\mathrm{f}} = {} & \frac{A'(T_{\mathrm{i}}) - K'(T)A(T_{\mathrm{i}})}{K'(T) + \sqrt{D_{\mathrm{S}}^{\mathrm{f}}/D_{\mathrm{P}}}}\mathrm{erfc}\frac{x}{2\sqrt{D_{\mathrm{S}}^{\mathrm{f}}t}} \\ & + \frac{[A'(T_{\mathrm{i}}) - K'(T)A(T_{\mathrm{i}})]\left(\sqrt{D_{\mathrm{S}}^{\mathrm{f}}/D_{\mathrm{P}}} - 1\right)}{[1 + K'(T)]\left[K'(T) + \sqrt{D_{\mathrm{S}}^{\mathrm{f}}/D_{\mathrm{P}}}\right]} \\ & \times \exp\left\{\frac{2}{d}\frac{1 + K'(T)\sqrt{D_{\mathrm{P}}/D_{\mathrm{S}}^{\mathrm{f}}}}{1 + K'(T)}x \right. \\ & \left. + D_{\mathrm{S}}^{\mathrm{f}}t\left[\frac{2}{d}\frac{1 + K'(T)\sqrt{D_{\mathrm{P}}/D_{\mathrm{S}}^{\mathrm{f}}}}{1 + K'(T)}\right]^2\right\} \\ & \times \mathrm{erfc}\left\{\frac{x}{2\sqrt{D_{\mathrm{S}}^{\mathrm{f}}t}} + \frac{2}{d}\frac{1 + K'(T)\sqrt{D_{\mathrm{P}}/D_{\mathrm{S}}^{\mathrm{f}}}}{1 + K'(T)}\sqrt{D_{\mathrm{S}}^{\mathrm{f}}t}\right\} \\ & + A(T_{\mathrm{i}}) \end{aligned} \tag{2}$$

$$\begin{aligned} C_{\mathrm{P}} = {} & \frac{[K'(T)A(T_{\mathrm{i}}) - A'(T_{\mathrm{i}})]\sqrt{D_{\mathrm{S}}^{\mathrm{f}}/D_{\mathrm{P}}}}{K'(T) + \sqrt{D_{\mathrm{S}}^{\mathrm{f}}/D_{\mathrm{P}}}}\mathrm{erf}\frac{x}{2\sqrt{D_{\mathrm{P}}t}} \\ & + \frac{[K'(T)A(T_{\mathrm{P}}) - A'(T_{\mathrm{P}})]K'(T)\left(1 - \sqrt{D_{\mathrm{S}}^{\mathrm{f}}/D_{\mathrm{P}}}\right)}{\left[1 + K'(T)\right][K'(T) + \sqrt{D_{\mathrm{S}}^{\mathrm{f}}/D_{\mathrm{P}}}]} \\ & \times \exp\left\{\frac{2}{d}\frac{K'(T) + \sqrt{D_{\mathrm{S}}^{\mathrm{f}}/D_{\mathrm{P}}}}{1 + K'(T)}x \right. \\ & \left. + D_{\mathrm{P}}t\left[\frac{2}{d}\frac{K'(T) + \sqrt{D_{\mathrm{S}}^{\mathrm{f}}/D_{\mathrm{P}}}}{1 + K'(T)}\right]^2\right\} \cdot \mathrm{erfc}\left\{\frac{x}{2\sqrt{D_{\mathrm{P}}t}} \right. \\ & \left. + \frac{2}{d}\frac{K'(T) + \sqrt{D_{\mathrm{S}}^{\mathrm{f}}/D_{\mathrm{P}}}}{1 + K'(T)}\sqrt{D_{\mathrm{P}}t}\right\} + A'(T_{\mathrm{i}}) \end{aligned} \tag{3}$$

where $C_{\mathrm{V}}^{\mathrm{f}}$, $C_{\mathrm{S}}^{\mathrm{f}}$ and C_{P} are the concentration of free vacancies, free solutes and solute-vacancy complexes respectively, $D_{\mathrm{V}}^{\mathrm{f}}$, $D_{\mathrm{S}}^{\mathrm{f}}$ and D_{P} the diffusion coefficient of free vacancies, free solutes and solute-vacancy complexes respectively; t is the time, x the distance from the grain boundary, d the thick of grain boundary (0.681 nm) [4], T_{i} initial equilibrium temperature and T temperature at which the diffusion is apparently inactive (for example, T can be set at 489 K for Ni_3Al [17], $A(T_{\mathrm{i}})$ and $A'(T_{\mathrm{i}})$ are initial concentration of solutes and complexes; $K'(T) = K(T)A''(T)$, where $K(T)$ is mass action constant, $A''(T)$ equilibrium concentration of vacancies at grain boundaries at temperature T.

4. Experimental and theoretical simulation results

Figs 1–6 show the grain boundary segregation profiles of boron and magnesium in Ni_3Al-0.0944at%B-0.0210at%Mg and Ni_3Al-0.0944at%B-0.0840at%Mg alloys from the temperatures of 1023, 1223 and 1373 K, and under the cooling rates of 0.05, 4.5 and 269 K/s. From the figures, it can be seen that the grain boundary segregation profiles of boron under the conditions mentioned above change smoothly with distance from the peak at grain boundaries and have a long enrichment tail of decreasing concentration. They are composed of two regions. In the first region, the boron concentration has a peak value at the grain boundary and decreases quickly to a low value as it is apart from the grain boundary within a short distance of 0.6–1 nm. In the second region, the boron concentration decreases slowly with a tail of lower concentration within a long distance of larger than 1.2 nm. Thus the shape of concentration profiles indicates that both processes of equilibrium and non-equilibrium segregation of boron take place simultaneously at grain boundary of Ni_3Al. The equilibrium segregation is dominant in the first segregation region and the non-equilibrium segregation in the second segregation. However, the grain boundary segregation profiles of magnesium change slightly with distance from a lower concentration at grain boundaries and have a long enrichment tail within a long distance of larger than 1.2 nm. The shape of concentration profiles indicates that the process of non-equilibrium segregation takes place at grain boundaries in Ni_3Al–B–Mg alloys. Compared with the grain boundary segregation profiles of boron in boron-doped Ni_3Al alloy (Ni_3Al-0.0944at%B) without the addition of magnesium (see Fig. 7), the magnesium addition can enhance the segregation concentration of boron at grain boundaries. There exists a grain boundary non-equilibrium co-segregation of boron and magnesium. It is found that the non-equilibrium grain boundary

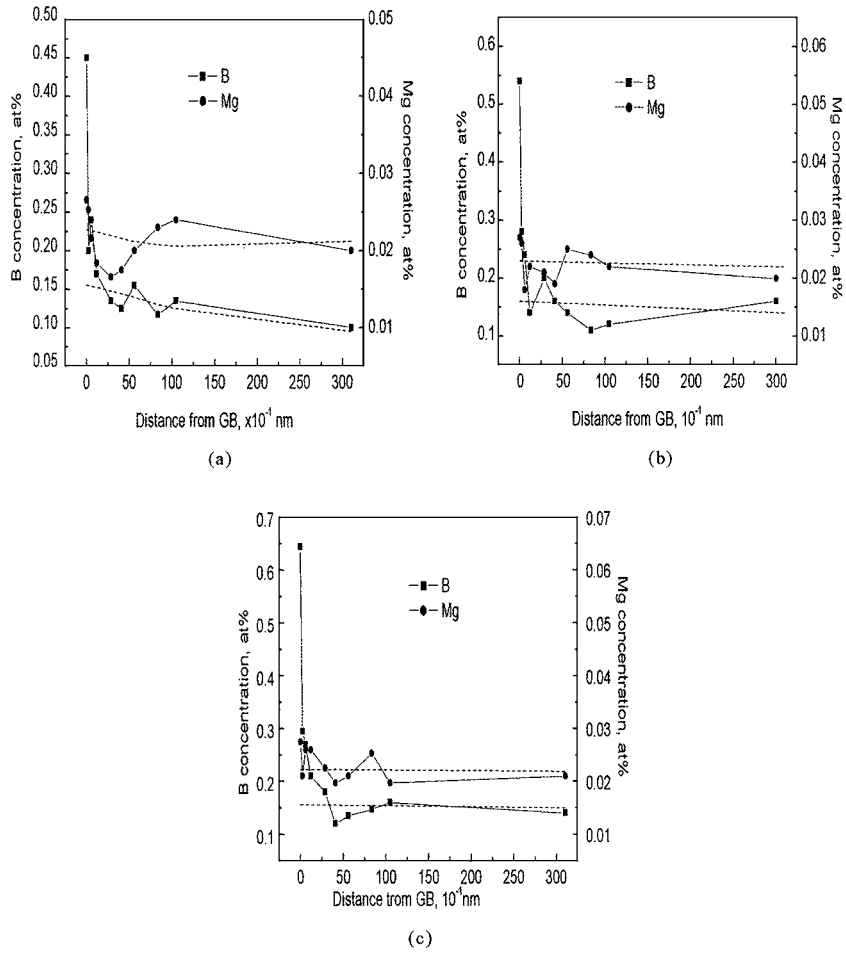

Figure 1 Experimental segregation profiles (solid line) and calculated segregation profiles (dashed line) in Ni_3Al with 0.0944at%B and 0.0210at%Mg. The starting temperature is 1373 K and the cooling rates are (a) 269 (b) 4.5 and (c) 0.05 K/s.

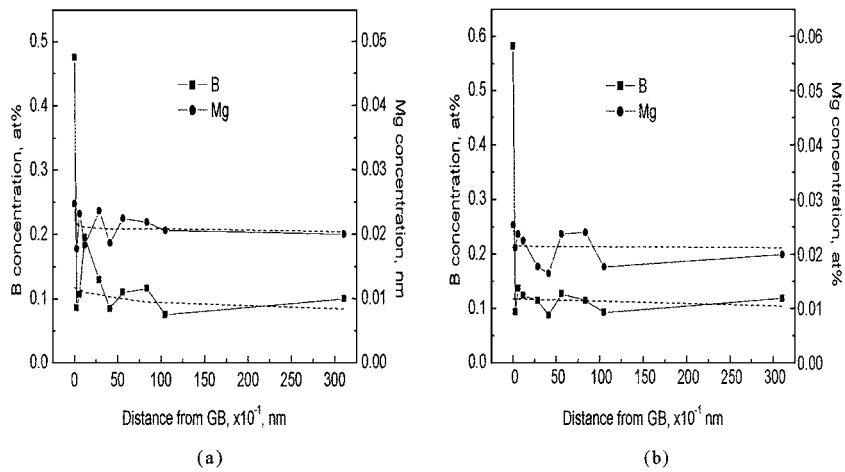

Figure 2 Experimental segregation profiles (solid line) and calculated segregation profiles (dashed line) in Ni_3Al with 0.0944at%B and 0.0210at%Mg. The starting temperature is 1223 K and the cooling rates are (a) 269 and (b) 4.5 K/s.

enrichment and the enrichment zone of boron and magnesium increase with increasing the initial temperature or decreasing the cooling rate. It is also shown that the grain boundary segregation concentration of boron increases, but that of magnesium decreases with increasing magnesium content.

The Equations 2 and 3 have been applied to fit the experimental data and to verify the theoretical expression. To determine the parameters of diffusion coefficients for boron and magnesium atoms, D_S^f and boron-vacancy complexes, D_P and binding energy of complexes, $E_{b(B)}$ an assumption was made that the diffusion frequency factor and binding energy of solute-vacancy complexes are equal to diffusion frequency factor of vacancy and diffusion activation of solute, respectively [13]. By adjusting these three parameters step by step, the segregation profiles were calculated (see Fig. 7). Good agreement between the experimental data and calculation for the non-equilibrium segregation of boron in boron-doped Ni_3Al is achieved [5, 8].

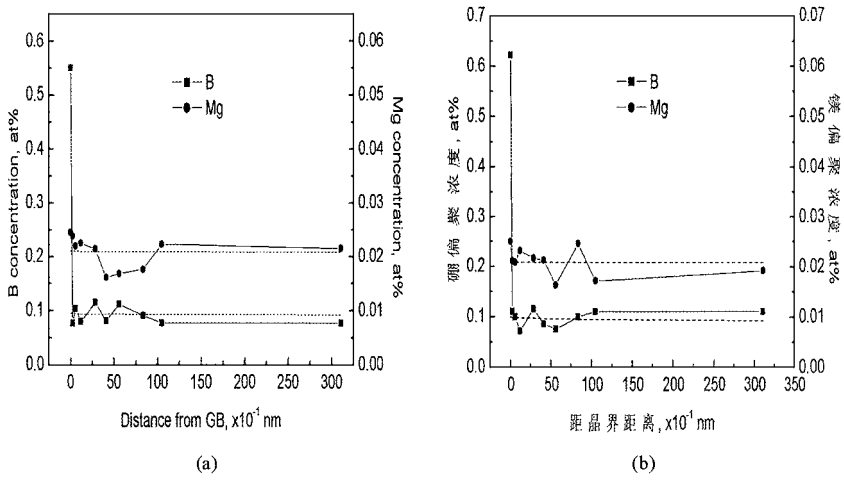

Figure 3 Experimental segregation profiles (solid line) and calculated segregation profiles (dashed line) in Ni_3Al with 0.0944at%B and 0.0210at%Mg. The starting temperature is 1023 K and the cooling rates are (a) 269 and (b) 4.5 K/s.

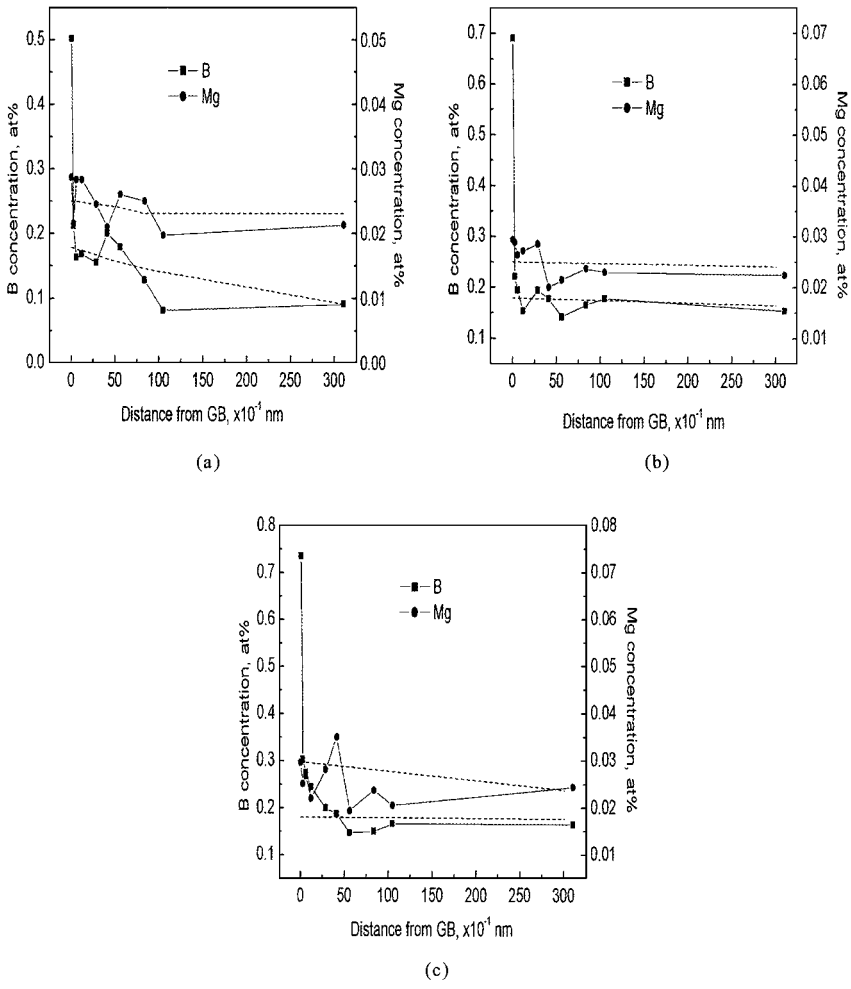

Figure 4 Experimental segregation profiles (solid line) and calculated segregation profiles (dashed line) in Ni_3Al with 0.0944at%B and 0.0840at%Mg. The starting temperature is 1373 K and the cooling rates are (a) 269 (b) 4.5 and (c) 0.05 K/s.

The diffusion coefficients for boron atom and boron-vacancy complexes were determined to be $D_B^f = 1 \times 10^{-6}$ exp[-1.96 (eV)/kT] and $D_{P(B)} = 1 \times 10^{-4}$ exp[-1.96 (eV)/kT] (m^2/s), respectively and the binding energy value of boron-vacancy complexes was estimated to be $E_{b(B)} = 0.5$ eV in boron-doped Ni_3Al [5, 8].

To simulate the grain boundary segregation of boron and magnesium in Ni_3Al–B–Mg alloys an assumption was made that the magnesium addition doesn't change the coefficients of boron atom and boron-vacancy complexes in boron-doped Ni_3Al. Thus the parameters to be determined are only the coefficients for magnesium, D_{Mg}^f and magnesium-vacancy, $D_{P(Mg)}$ and binding energy of boron-vacancy, $E_{b(B)}$ and magnesium-vacancy, $E_{b(Mg)}$. By adjusting these four parameters step by step, the non-equilibrium segregation profiles were calculated and are shown as dashed lines in the Figs 1–6. There is good agreement

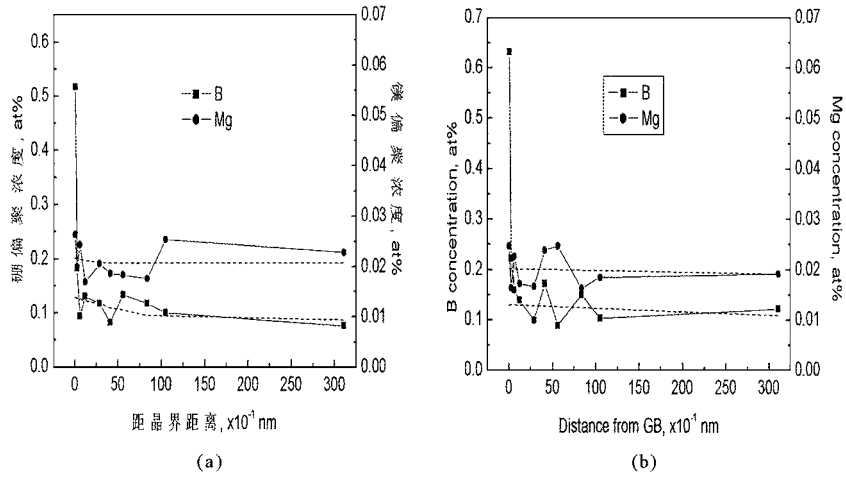

Figure 5 Experimental segregation profiles (solid line) and calculated segregation profiles (dashed line) in Ni_3Al with 0.0944at%B and 0.0840at%Mg. The starting temperature is 1223 K and the cooling rates are (a) 269 and (b) 4.5 K/s.

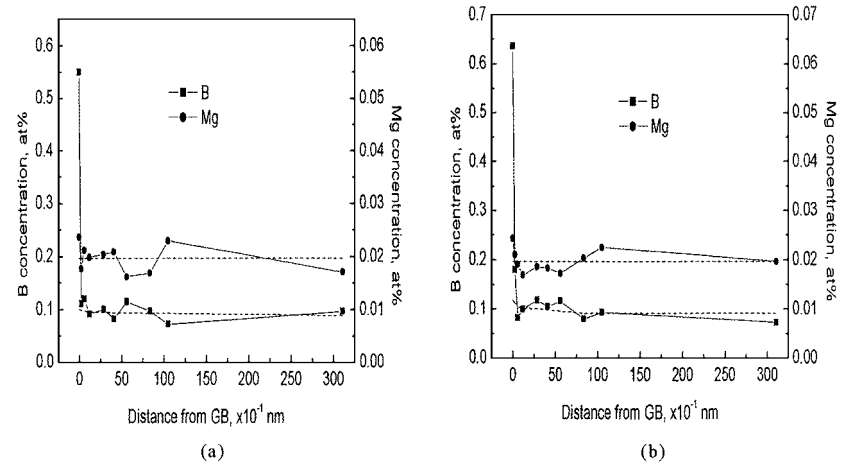

Figure 6 Experimental segregation profiles (solid line) and calculated segregation profiles (dashed line) in Ni_3Al with 0.0944at%B and 0.0840at%Mg. The starting temperature is 1023 K and the cooling rates are (a) 269 and (b) 4.5 K/s.

between the experimental data and calculation for the non-equilibrium segregation of boron and magnesium in Ni_3Al—B—Mg alloys. The diffusion coefficients for magnesium and magnesium-vacancy were determined to be $D^{f}_{Mg} = 4.4 \times 10^{-6}\ \exp[-2.52\ (\mathrm{eV})/kT]$ and $D_{P(Mg)} = 1 \times 10^{-4} \exp[-2.52\,(\mathrm{eV})/kT]\,(\mathrm{m^2/s})$, respectively, where the frequency factor was taken from the diffusion data of magnesium in pure nickel [18], that is $D_{0(Mg)} = 4.4 \times 10^{-6}\ \mathrm{m/s^2}$. The binding energy value of magnesium-vacancy and boron-vacancy complexes was estimated to be $E_{b(B)} = 0.66$ eV for Ni_3Al-0.0944at%B-0.0210at%Mg alloy and $E_{b(B)} = 0.71$ eV for Ni_3Al-0.0944at%B-0.0840at%Mg alloy. Compared with $E_{b(B)} = 0.5$ eV for boron-doped Ni_3Al without magnesium addition, the magnesium addition can increase the binding energy of boron-vacancy complexes, which will lead to enhance grain boundary segregation of boron in boron-doped Ni_3Al alloys.

5. Discussion

In this paper, the experimental results combined with the theoretical simulations indicate that both equilibrium and non-equilibrium segregation of boron and non-equilibrium segregation of magnesium exist at the grain boundary in Ni_3Al. There exists the grain boundary non-equilibrium co-segregation of boron and magnesium in Ni_3Al—B—Mg alloys. Moreover, the moderate attractive interactions between boron and magnesium can give rise to an increase in the binding energy of boron-vcancy, which leads to enhance grain boundary segregation of boron.

The correctness of quantitative description for non-equilibrium segregation of boron and magnesium depends on the correct determination of parameters needed for the theoretical calculation in this study. Under the condition of complete segregation profiles measured experimentally the parameters needed for theoretical fitting to experimental profiles can be determined uniquely. However, the completeness of experimental segregation profiles cannot be obtained from the limitation of experimental conditions. In this paper, to determine the parameters of diffusion coefficients for boron and magnesium atoms, boron-vacancy and magnesium-vacancy complexes and binding energy of complexes, an assumption was made that the diffusion frequency factor and binding energy of solute-vacancy complexes are equal to the diffusion frequency factor of vacancy and diffusion activation energy of solute, respectively, which simplifies the condition for the parameter determination. From the discussion above, it is necessary to verify the complex diffusion mechanisms

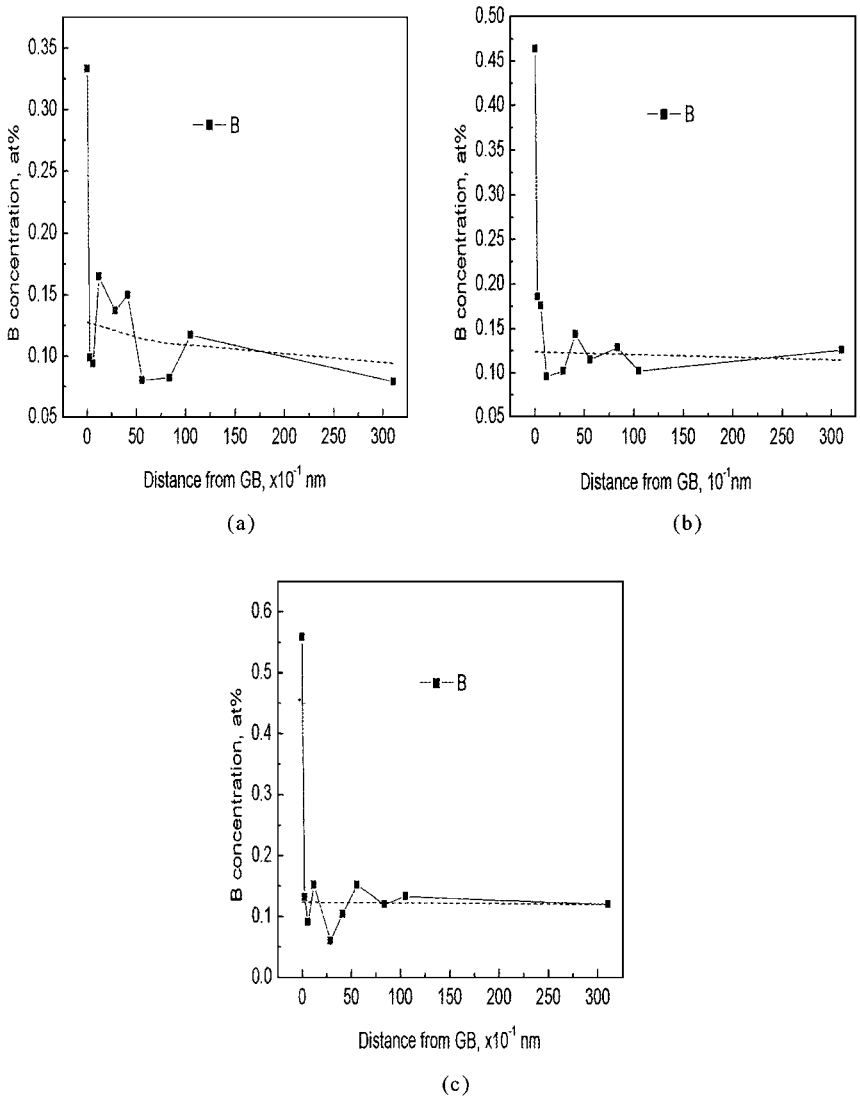

Figure 7 Experimental segregation profiles (solid line) and calculated segregation profiles (dashed line) in Ni_3Al with 0.0944at%B. The starting temperature is 1373 K and the cooling rates are (a) 269 (b) 4.5 and (c) 0.05 K/s.

for quantitative description of non-equilibrium segregation. However, limited work has been done in this aspect [19, 20]. Recently, Choudhury *et al.* [4] estimated the diffusion activation energy of boron in Ni_3Al to be a range of 2.07–3.11 eV from the equilibrium segregation kinetics treatment. In this paper, the diffusion activation energy of boron was determined to be 1.96 eV, which is a reasonable value.

6. Conclusion

1. Both equilibrium and non-equilibrium grain boundary segregation of boron and non-equilibrium grain boundary segregation of magnesium in Ni_3Al–B–Mg alloys were determined by AES in conjunction with ion sputtering in a cooling rate range of 0.05–286.91 K/s and an initial temperature range of 1023–1373 K. The grain boundary segregation enrichment and enrichment zone increase with increasing initial temperature and decreasing cooling rate.

2. There exists a grain boundary non-equilibrium co-segregation of boron and magnesium in Ni_3Al–B–Mg alloys. The magnesium addition can increase the binding energy of boron, which leads to enhanced grain boundary segregation of boron in boron-doped Ni_3Al alloys.

3. The analytical expressions of diffusion rate equations describing non-equilibrium segregation process based on the concept that mobile solute-vacancy complexes migrating to grain boundaries (vacancy sinks) is responsible for the grain boundary non-equilibrium segregation of solute atoms in an alloy were used to simulate well the experimental segregation profiles of boron and magnesium in Ni_3Al–B–Mg alloys. The diffusion coefficients for boron atoms and boron-vacancy complexes in Ni_3Al–B alloys were determined to be $D_B^f = 1 \times 10^{-6} \exp[-1.96\ (\mathrm{eV})/kT]$ and $D_{P(B)} = 1 \times 10^{-4} \exp[-1.96\ (\mathrm{eV})/kT]$ (m^2/s), respectively, and the binding energy value of boron-vacancy complexes was estimated to be $E_{b(B)} = 0.5$ eV. The diffusion coefficients for magnesium atoms and magnesium-vacancy complexes in Ni_3Al–B–Mg alloys were determined to be $D_{Mg}^f = 4.4 \times 10^{-6} \exp[-2.52\ (\mathrm{eV})/kT]$ and $D_{P(Mg)} = 1 \times 10^{-4} \exp[-2.52\ (\mathrm{eV})/kT]$ (m^2/s), respectively, and the binding energy value of magnesium-vacancy and boron-vacancy complexes was estimated to be $E_{P(Mg)} = 0.67$ eV, $E_{b(B)} = 0.66$ eV (for 0.0210at%Mg) and $E_{b(B)} = 0.71$ eV (for 0.0840at%Mg).

Acknowledgement

This work was supported by National Natural Science Foundation of China and National Advanced Materials Committee of China.

References

1. C. T. LIU, C. L. WHITE and J. A. HORTON, **33** (1985) 213.
2. A. CHOUDHURY, C. L. WHITE and C. R. BROOKS, *Scr Metall* **20** (1986) 1061.
3. DONGLIANG LIN and DA CHEN, *Acta Metall. Mater.* **38** (1990) 523.
4. A. CHOUDHURY, C. L. WHITE and C. R. BROOKS, *ibid.* **40** (1992) 57.
5. YUN ZHANG and DONGLIANG LIN, *Transactions of Metal Heat Treatment* **17** (Suppl.) (1996) 32.
6. YIMING WANG, DONGLIANG LIN and ZHANG YUN, in Mater Res Soc Symp Proc, Vol. 460, edited by Carl C. Koch, C. T. Liu, N. Stoloff and A. Wanner (Mater. Res. Soc., Pittsburgh, PA, USA, 1997) p. 511.
7. DONGLIANG LIN and YUN ZHANG, in proceedings of JIMIS-8, edited by Y. Ishida, M. Morita, T. Suga, H. Ichimose, O. Ohashi and J. Echigoya, (The Japan Institute of Metals, 1997), p. 53.
8. *Idem.*, *Mater Sci Eng* **256A** (1998) 39.
9. C. C. CHANG, *Surface Sci.* **48** (1975) 9.
10. S. ICHIMURS and R. SCHIMIZU, *ibid.* **112** (1981); **115** (1982) 259.
11. T. SEKINE, K. HIRATA and AMOGAMI, *ibid.* **126** (1983) 565.
12. YUN ZHANG and DONGLIANG LIN, *Physical testing and Chemical Analysis, Part A: Physical Testing* **33**(1) (1997) 22.
13. T. M. WILLIAMS, A. M. STONEHAM and D. K. HARRIES, *Met. Sci. J.* **10** (1976) 14.
14. X. L. HE and Y. T. CHU, *J. Phys. D, J. App. Phys.* **16** (1983) 1145.
15. M. A. V. CHAPMAN and R. G. FAULKNER, *Acta Metall.* **31** (1983) 677.
16. L. KARSSON, *ibid.* **38** (1988) 35.
17. T. M. WANG, M. SHIMOTOMAI and M. DOYAMA, *J. Phys. F, Met. Phys.* **14** (1984) 37.
18. P. R. A. SWALIN, A. MARTIN and R. OLSEN, *Trans. AIME* **209** (1957) 936.
19. G. SCHEWMON, "Diffusion in Solids" (McGraw-Hill Book Company, Inc, New York, 1990) p. 115.
20. ZHONGSHENG YU and NING CHEN, *Science in China* A **10** (1992) 1114.

Received 28 May
and accepted 2 July 2002